Recent Advances in Salt-Template Assisted Synthesis of 3D Porous Carbon Materials for Electrochemical Energy Storage

Cao Jiang[+, a] Huawei Liu[+, a, b] Jingzhe Ye[+, a] Ning Wang,[d, e] Ying Tang,[b] Chunnian He,[a, b, c] Haichang Zhang,*[d, e] and Biao Chen*[a, b]

The structure, morphology, and composition of electrode materials play a crucial role in determining the electrochemical performance of energy storage devices. Among various materials, three-dimensional (3D) porous carbon stands out for its potential to enhance electrochemical energy storage due to its cost-effectiveness, excellent ion and electron conductivity, abundant active sites, and customizable pore structure. The salt-template method offers an environmentally friendly, fast, and cost-efficient approach to synthesizing 3D porous carbon, with the added advantage of adjustable pore architecture and composition. This review provides a comprehensive overview of recent advancements in preparing 3D porous carbon and its composites using the salt-template method, emphasizing their applications in batteries and supercapacitors. It also critically examines the existing challenges and explores potential future directions for further development in this field.

1. Introduction

The demand for safe, low-cost, and efficient electrochemical energy storage devices (EESDs) has become more urgent as the need to develop sustainable development of future energy grows ever stronger.[1] Carbon materials are desirable candidates as electrode materials of EESDs due to their abundant availability, low toxicity, and versatile structure. In recent years, a variety of carbon materials and their composites with diverse structures have been constructed including zero-dimensional (0D) fullerenes and carbon spheres, one-dimensional (1D) carbon nanotubes, and carbon nanofibers, two-dimensional (2D) graphene and carbon sheets, 3D graphene foams and porous carbon.[2] Among them, 3D carbon materials stand out for their high specific surface area, excellent electrical conductivity, rich porous

structure, and commendable structural stability.[3] These characteristics make 3D carbon materials highly effective in a wide range of electrochemical applications, from active materials to conducting agents and substrates in EESDs.

To achieve 3D porous carbon with diverse pore structures, researchers have increasingly focused on developing rapid and environmentally friendly preparation methods. The template method has emerged as a primary approach for fabricating porous carbon materials due to its simplicity and efficiency. This method can be categorized into two types based on the templates used: hard template and soft template.[4] The hard template method, in particular, offers better controllability and facilitates the formation of stable structures with vertical channels.[5] Commonly used templates include metals, metal compounds, and water-(in)soluble inorganic salts.[6] Among these, water-soluble inorganic salts have outstanding advantages in the template method because of their cost effectiveness, environmental friendliness, and recyclability, consistent with the global sustainable development goals of energy.

As a result, the fabrication of 3D porous carbon using salt-templating techniques for various EESDs has gained significant attention in recent years. This review focuses on recent design and fabrication strategies of various 3D carbon materials and their composites, with an emphasis on their applications in EESDs, particularly highlighting contributions from Tianjin University of China. The salt template synthesis method is simple in operation and simple in experimental equipment and can be used to design the structure, pore size and morphology of three-dimensional porous carbon and its composites. And it has outstanding advantages as the electrode material of batteries and capacitors, reflecting good performance. This work summarizes the unique design of 3D porous carbon in recent years and its application in the field of energy storage, which can provide a certain reference

[a] C. Jiang,+ H. Liu,+ J. Ye,+ C. He, B. Chen
     School of Materials Science and Engineering, Tianjin Key Laboratory of Composite and Functional Materials, Key Laboratory of Advanced Ceramics and Machining Technology (Ministry of Education), Tianjin University, Tianjin 300350, People's Republic of China
     E-mail: bchen@tju.edu.cn

[b] H. Liu,+ Y. Tang, C. He, B. Chen
     National Industry-Education Platform of Energy Storage, Tianjin University, Tianjin, 300350, People's Republic of China

[c] C. He
     Joint School of National University of Singapore and Tianjin University, International Campus of Tianjin University, Binhai New City, Fuzhou, 350207, People's Republic of China

[d] N. Wang, H. Zhang
     State Key Laboratory of Reliability and Intelligence of Electrical Equipment, Hebei University of Technology, Tianjin, 300401, People's Republic of China
     E-mail: hczhang@hebut.edu.cn

[e] N. Wang, H. Zhang
     School of Electrical Engineering, Hebei University of Technology, Tianjin, 300401, People's Republic of China

[+] These authors are co-first authors

Batteries & Supercaps

Review
doi.org/10.1002/batt.202400563

Chemistry Europe
European Chemical
Societies Publishing

for the design of 3D porous carbon synthesis by salt template method in the future.

2. Salt-Templating Synthesis

It is well known that the morphology, pore size, and pore distribution of 3D porous carbon have a great influence on the performance of electrode materials. These are directly related to the selection and parameters of the salt template, when the salt template is removed, its original position will leave the corresponding size of the hole. Therefore, the parameters of porous carbon can be directly controlled by selecting the type and quantity of salt template. The synthesis of 3D porous carbon using a sacrificial template involves two key steps. First, a water-soluble salt (such as NaCl, KCl, Na_2CO_3, or Na_2SO_4) is used as a template, with carbonaceous precursors filling its framework.[7] This step typically involves a self-assembly process. Following this, the self-assembled, carbonized template is removed through chemical etching or water washing, resulting in the formation of porous carbon materials.[8] The assembly process of the water-soluble salt templates and organic precursors is particularly critical, as it largely determines the structure and morphology of the final 3D porous carbon

2.1. Self-Assembly Strategies

Figure 1a illustrates three current self-assembly methods: low-temperature freeze-drying, room-temperature anti-solvent, and high-temperature spray drying. Zhao et al. developed a technique for preparing 3D porous carbon precursors using low-temperature freeze-drying with various multi-scale inorganic sodium salts (Figure 1b and c).[9,10] In this process, the glucose and the three NaX salts (X: Cl^-, CO_3^{2-}, SO_4^{2-}) were dissolved in deionized water to form a uniform solution, which was then freeze-dried to remove the moisture in it. The presence of different types of inorganic salts leads to the formation of multi-scale salt particles ranging in size from nanometers to microns. These salt particles are coated in glucose and self-assemble into complex 3D structures. The glucose is then carbonized, forming a composite material of multi-scale salt particles coated with carbon. Finally, the solid powder is treated with distilled water to remove the template, yielding pure 3D porous carbon material. By adjusting and combining different salt templates, both the specific surface area and pore size distribution of the resulting 3D carbon structure can be tailored, making this method suitable for the custom synthesis of 3D porous carbons

Another method, high-temperature spray-drying, enables rapid self-assembly of salt templates with a carbon source for

Cao Jiang obtained his B. E. degree from Harbin Engineering Uninversity in 2020 and M. E. at Chongqing Key Laboratory for Battery Materials and Technology, Southwest University in June of 2024. His research focuses on electrode materials for Na-ion batteries and cycling of cathode materials from spent lithium-ion batteries.
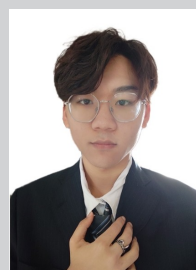
Huawei Liu is currently a master student at the School of Materials Science and Engineering, Tianjin University. He received his bachelor degree from Hebei University of Technology in 2024. His research interests focus on machine learning to guide the synthesis and development of new materials.

Jingzhe Ye is currently a master student at the School of Materials Science and Engineering, Tianjin University. He received his bachelor degree from Hefei University of Technology in 2024. His research interests focus on the electrode materials of lithium-ion batteries.

Haichang Zhang obtained his B.S. and M.S. degrees from Nankai University in 2002 and 2005, respectively, and his Ph.D. from Tianjin University in 2022. From 2005 to 2023, he worked at the "Science and Technology on Power Sources Laboratory" of "Tianjin Institute of Power Sources". In 2023, he joined the School of Electrical Engineering at Hebei University of Technology as a Professor. His current research is focused on synthesis and fabrication of electrode materials for rechargeable batteries.

Biao Chen is currently an associate professor at the School of Materials Science and Engineering, at Tianjin University. He received his PhD degree in Materials Science in 2020 from Tianjin University under the supervision of Prof. Naiqin Zhao and Prof. Shi-Zhang Qiao. He worked as a postdoctoral fellow at Tsinghua Shenzhen International Graduate School, Tsinghua University from 2020 to 2022, with Prof. Hui-Ming Cheng and Prof. Guangmin Zhou. His research interest mainly focuses on lithium-ion battery recycling next-generation conversion-type batteries, including sodium-ion batteries, sodium-CO_2 batteries, and sodium-sulfur batteries. He is the Associate Editor of the Journal of Materials Science and Discover Applied Sciences.

Batteries & Supercaps

Review
doi.org/10.1002/batt.202400563

Chemistry Europe
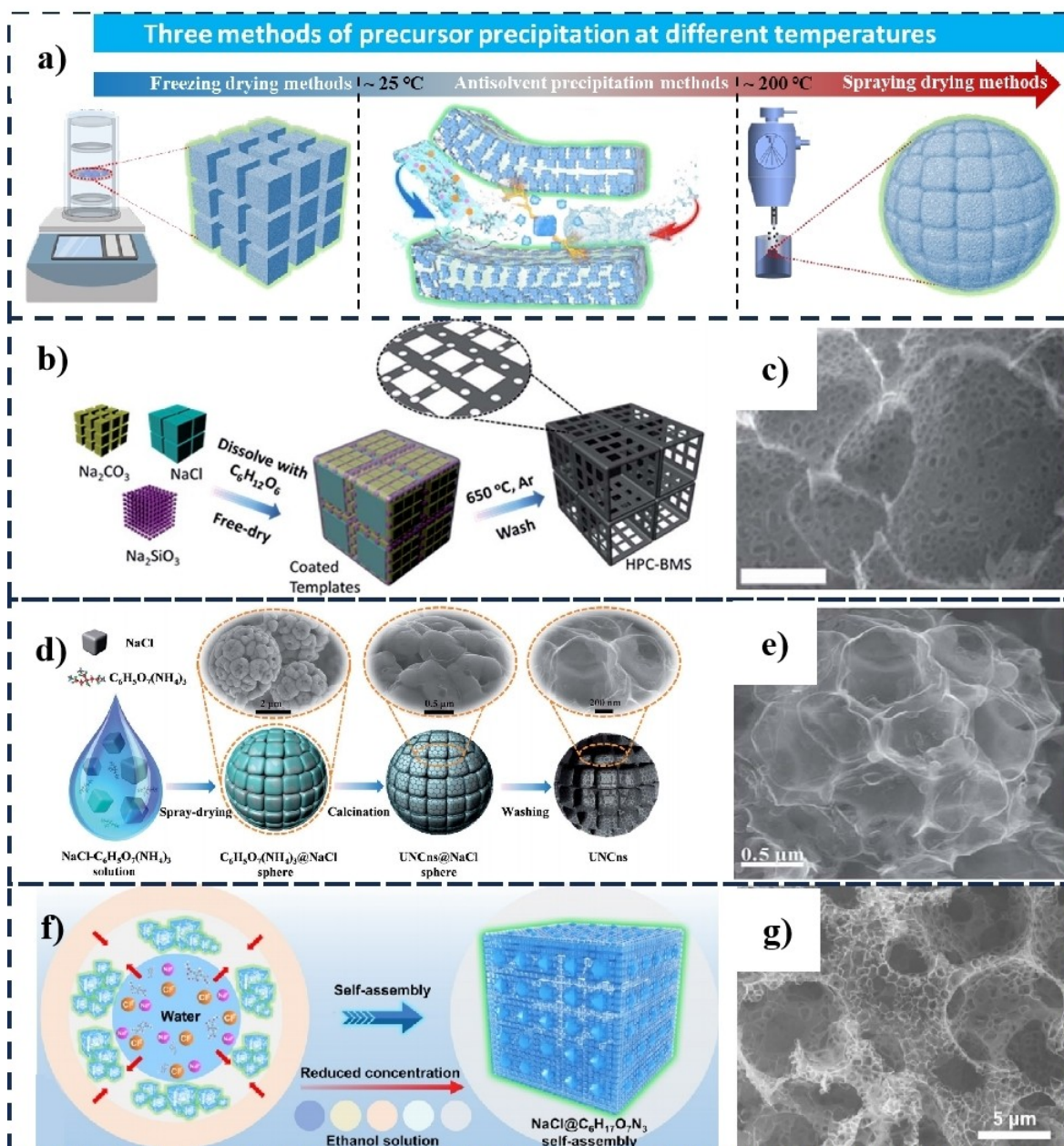European Chemical
Societies Publishing

Figure 1. (a) Schematic diagrams of the current salt-template self-assembly methods. Reproduced with permission.[9] Copyright 2023, Wiley-VCH GmbH. (b) Schematics demonstrating the fabrication process and (c) SEM image of 3D hierarchical porous carbons. Reproduced with permission.[10] Copyright 2015, The Royal Society of Chemistry. (d) Schematic illustration of the synthesis and (e) SEM image of N-doped interconnected carbon spheres with ultrathin nanosheets. Reproduced with permission.[11] Copyright 2019, The Royal Society of Chemistry. (f) Mechanism diagram of the antisolvent precipitation process and (g) SEM image of nitrogen-doped 3D porous carbon. Reproduced with permission.[9] Copyright 2023, Wiley-VCH GmbH.

the synthesis of 3D porous carbon. Li et al. used a simple template-assisted spray pyrolysis method to prepare N-doped interconnected carbon spheres with ultrathin nano-sheets and extended face spacing (Figure 1d and e).[11] They employed NaCl as a non-destructive and easily removable template to construct the spherical interconnected carbon network. NaCl and $C_6H_17N_3O_7$ were mixed with water to form a homogeneous solution, which was then spray-dried. During this process, the solution was dispersed into small droplets, and NaCl crystallized into nanocubes at high temperature, with an ultrathin layer of $C_6H_17N_3O_7$ encapsulating the

surface. The $C_6H_17N_3O_7@NaCl$ nanocubes inherited the shape of the droplets, self-assembling them into a spherical structure that formed an interconnected carbon network. This network ensures fast electron transport, while the mesoporous and N-doped properties enhance capacitance-controlled energy storage. This approach is versatile, extending beyond the construction of porous 3D carbon materials to other material systems.

While low-temperature freeze-drying and high-temperature spray-drying are widely used for self-assembly synthesis, both methods have drawbacks, such as equipment dependence and

Batteries & Supercaps

Review
doi.org/10.1002/batt.202400563

Chemistry
Europe

European Chemical
Societies Publishing

high energy consumption. To address these issues, more economical and environmentally friendly self-assembly synthesis methods that can be performed at room temperature are needed. As shown in Figure 1f and g, Chen et al. developed a room-temperature method for the self-assembly of precursors from salt templates and carbon source aqueous solutions interacting with anti-solvents.[9] This method takes advantage of the differing solubilities of salt templates and carbon source organics in water and industrial ethanol. The effects of various factors, including carbon sources, salt types, salt granularity, and the water-to-ethanol volume ratio, on structural parameters such as carbon yield and precursor volume size were systematically investigated. This approach allows for the effective synthesis of carbon and its composites (including metals, nitrides, carbides, and sulfides) with controllable aperture sizes at room temperature. Notably, this method does not rely on specialized equipment, and the anti-solvent can be recycled, making it both economical and environmentally sustainable.

2.2. Self-Standing Morphology Regulation

After self-assembly, the final 3D porous carbon material is typically obtained through high-temperature pyrolysis and water washing. However, materials synthesized at room temperature and atmospheric pressure often result in powder forms, which are prone to agglomeration and are unfavorable for ion transport (Figure 2a and c).[12] Consequently, there has been significant interest in designing strategies to prevent the agglomeration of 3D carbon materials. A common approach is to create self-standing electrodes by hot-pressing the 3D carbon or combining it with a metal matrix or other materials.

He et al. developed a method to embed sub-10 nm metal-based nanomaterials in self-supported carbon foams (SMNs) by overcoming the interfacial constraints of NaCl self-assembly and the thermo-mechanical coupling of powder metallurgical hot pressing (Figure 2d and f).[12a] In this process, NaCl was used as a template, and citric acid served as the carbon source, combined with metal compounds to produce precursor gels through freeze-drying. The resulting
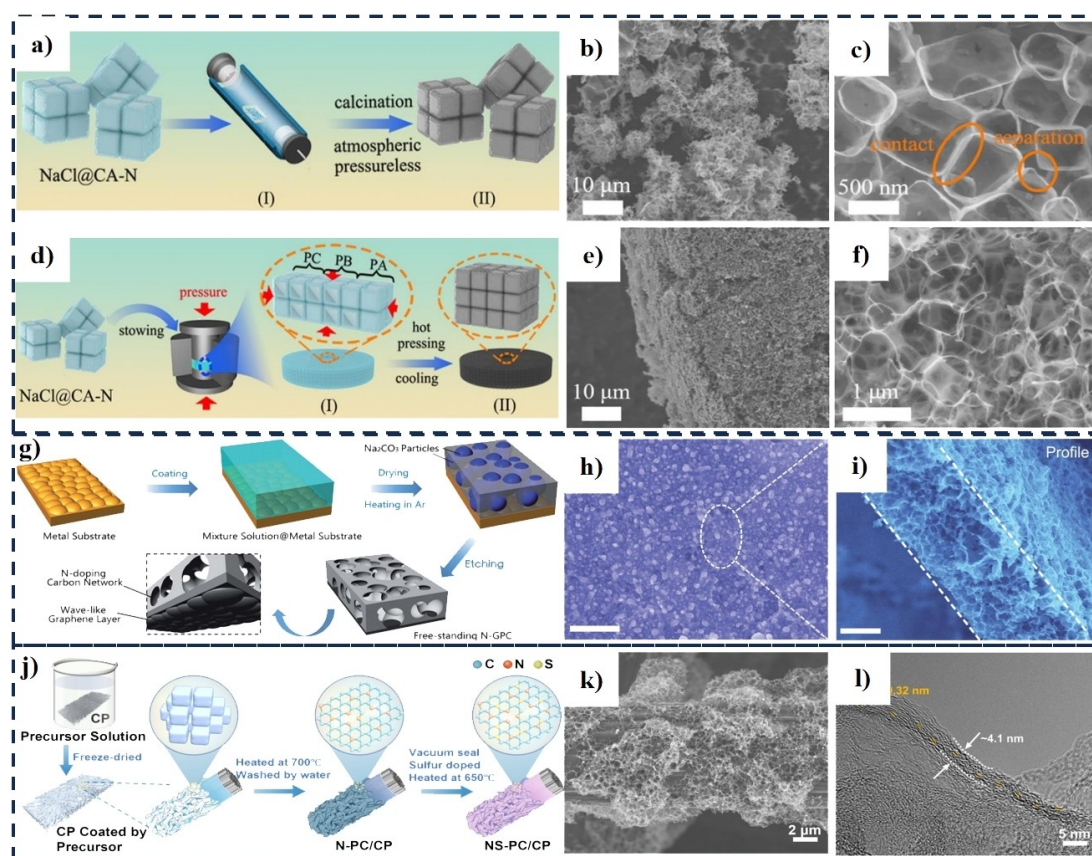

Figure 2. (a) Schematic illustration of the preparation processes and (b, c) SEM images of porous carbon powder. (d) Schematic illustration of the preparation process and (e, f) SEM images of free-standing carbon foam. Reproduced with permission.[12a] Copyright 2023, Wiley-VCH GmbH. (g) Schematic illustration of the synthesis process and (h, i) SEM images of N-doping porous carbon network /graphene layer. Reproduced with permission.[13] Copyright 2017, The Royal Society of Chemistry. (j) Schematic of the synthesis process and (k) SEM image and (l) HRTEM image of N, S co-doped porous carbon/carbon paper. Reproduced with permission.[14] Copyright 2024, Elsevier B.V.

Batteries & Supercaps

Review
doi.org/10.1002/batt.202400563

Chemistry Europe
European Chemical
Societies Publishing

citric acid and metal compound precursors network were distributed at the interfaces of the NaCl self-assembly (NaCl@CA-MCP–N). The obtained powders were then pressed into dense agglomerates within a circular graphite mold, followed by hot pressing and sintering under an external pressure of 30 MPa. By comparing the products obtained after heat treatment under both atmospheric and pressurized conditions, it was found that pressure-enhanced NaCl self-assembled interfacial confinement effectively prevented SMN agglomeration and facilitated the embedding of SMNs by welding carbon nanosheets into the free-standing carbon foam structure (FC–Fs). The citric acid networks and metal compounds were transformed into self-standing carbon foams and SMNs, respectively. After water washing to remove the NaCl templates, the embedded FC–Fs within the SMNs were obtained, which could be directly cut into electrodes of suitable size. The prepared SMN/FC–Fs exhibited independent structures, excellent mechanical properties, porous network structures, good electrical conductivity, and strong interfacial interactions.

In addition to pressurization, utilizing a composite design that incorporates 3D porous carbon grown on a suitable substrate offers a straightforward and effective approach for fabricating self-standing materials. Zhao et al. demonstrated this by using a solution of sodium carbonate, glucose, and urea, which was coated onto a metal substrate (Figure 2g–i).[13] Upon heating, the organic complexes converted into N-doped porous carbon networks, replicating the salt template pattern. Additionally, corrugated graphene formed in the gap between the metal and the salt, resulting in a structure with both 2D and 3D characteristics. This dual-structure not only enhances overall electronic conductivity but also improves the material's structural stability, providing it with an independent, self-standing character.

Further advancing this approach, Zhao et al. developed a self-supported Na-CO_2 battery electrode material consisting of a porous carbon mesh grown vertically on the surface of independent carbon paper (Figure 2j–l).[14] This was achieved through a combination of the salt-template method and a vacuum-sealed vulcanization process. The free-standing electrode's framework was constructed using superhydrophilic carbon paper (SH-CP), characterized by a reticulated structure and a high degree of carbonization. An ultrathin reticular structure of N-doped porous carbon (N–PC) was then grown in situ on the surface of SH-CP (N–PC/CP) using the salt-template method. Following this, a substantial amount of sulfur was further doped into the N–PC via vacuum-sealed vulcanization. As observed from the morphology, the porous carbon thoroughly covered the surface of the carbon cloth, ensuring close interactions. As the cathodes of Na-CO_2 batteries, the in situ-grown porous carbon network of the electrodes offers significant advantages in electrolyte and CO_2 diffusion and provides high-speed electron and ion transfer pathways.

3. Application for Batteries

As a current focal point in cathode material research, 3D porous carbon materials are extensively used in batteries due to their high specific surface area and outstanding conductivity, which facilitate efficient electron transport pathways in electrochemical reactions. The primary roles of 3D porous carbon materials in alkali metal batteries include participation as active materials in chemical reactions,[15] enhancing conductivity,[2c] and serving as catalyst supports.[16]

3.1. Alkali Metal Ion Batteries

3D porous carbon materials offer significant application potential in alkali metal batteries, yet their application in alkali metal ion batteries is primarily hindered by poor cycle stability. The pore size of 3D porous carbon is influenced by the type of salt template used, making precise control over pore structure and size challenging. This often results in the formation of SEI films, which increase internal resistance and reduce capacity. Besides, structural instability poses a significant challenge. The materials may undergo volume changes during repeated charge-discharge cycles, leading to structural damage and severely impacting cycle performance. To address these issues, researchers have proposed several strategies. Alloying and carbon coating have been developed to alleviate the volume expansion of active materials during the charge-discharge cycles.[2c] In addition, the use of high-entropy alloys for electrode fabrication has been suggested.[15] These approaches have shown some improvement in the cycle stability of alkali metal ion batteries.

Nitrogen doping is a prevalent technique for modifying 3D carbon materials. It introduces additional electrons, enhancing the conductivity of the carbon material. Furthermore, nitrogen doping alters the electronic structure, creating more active sites on the surface, optimizing catalytic performance in redox reactions, reducing dendrite formation, and ultimately improving cycle stability. This enhancement is attributed to nitrogen atoms narrowing the bandgap in carbon materials, thereby increasing their electrocatalytic activity. Bearing the aforementioned considerations in mind, Chen et al. introduced a 3D porous carbon (N-3DPC) material that improves cycle stability through nitrogen doping (Figure 3a) and controlled pore structure (Figure 3b), featuring a continuous pore size distribution ranging from micropores to macropores.[9] Nitrogen doping introduces additional electrons, altering the carbon layer structure and expanding the carbon layer spacing (Figure 3c). Furthermore, nitrogen doping modifies the defect density (Figure 3d), optimizing ion diffusion pathways and reducing ion transport resistance. This enables the N-3DPC material to better accommodate volume changes during charge and discharge cycles, minimizing structural damage and enhancing the efficiency and stability of the battery's electrochemical reactions. Besides, the Galvanostatic intermittent titration technique (GITT) measurement (Figure 3e) indicated that the N-3DPC material
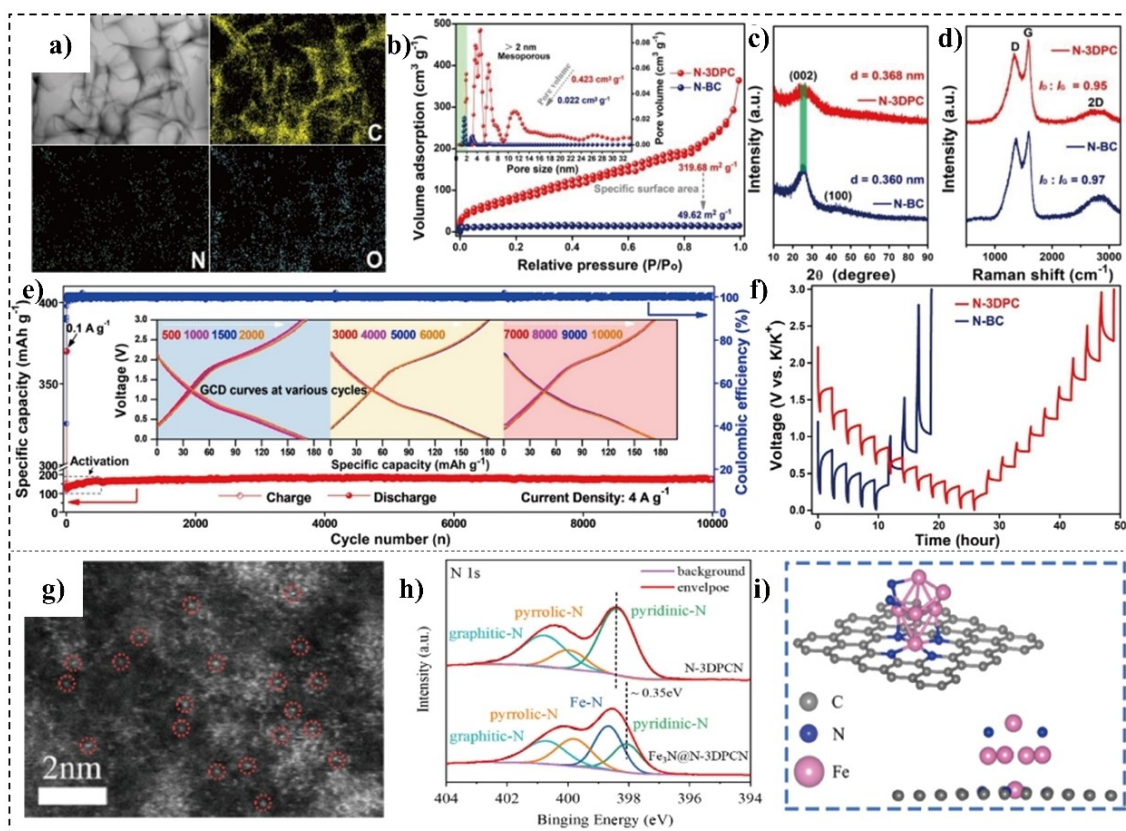
Figure 3. (a) STEM image of N-3DPC and corresponding EDS mappings of C, N, and O elements. (b) Nitrogen adsorption-desorption isotherms and the inset in (b) is the corresponding pore size distribution; (c) XRD patterns; and (d) Raman spectra of N-3DPC and N doped bulk carbon (N-BC). (e) Long-term cycle stability of N-3DPC at a high current density of 4 A g^{-1}, and the corresponding GCD curves at different circles (illustration). (f) GITT profiles of N-3DPC and N-BC. Reproduced with permission.[9] Copyright 2023, Wiley-VCH GmbH. (g) AC-STEM-ADF images of fully sodiated Fe$_3$N@N-3DPCN after 500 cycles at 500 mA g^{-1}, the red circles stand for Fe single atoms, and the green circles indicate Fe. (h) High-resolution XPS N 1s spectra of N-3DPCN and Fe$_3$N@N-3DPCN. (i) The atomic structures of Fe$_3$N adsorbed on quadra-pyridinic-N doped graphene. Reproduced with permission.[7c] Copyright 2022, Elsevier Ltd.

has a high potassium ion diffusion coefficient during the charge-discharge process, confirming the reduction of battery polarization effects. Long-term cycling tests further demonstrate that the N-3DPC material maintains a high reversible capacity of 176 mAh g^{-1} after 10,000 cycles at a current density of 4 A g^{-1}, with a capacity decay rate of just 0.01% per 100 cycles, indicating excellent cycle stability even at high rates. The Galvanostatic charge-discharge (GCD) profiles also exhibit good overlap and minimal polarization (Figure 3f). This outstanding long cycling stability is attributed to the material's high specific surface area, abundant defect sites, well-structured pores, and large carbon layer spacing.

Additionally, Liang et al. reported a composite of isolated ultrafine Fe$_3$N nanocrystals (<15 nm) strongly coupled with N-doped 3D porous carbon networks (N-3DPCN) (Figure 3g).[7c] Both experimental results and theoretical simulations have validated that the interfacial interaction between Fe$_3$N and N-3DPCN is strongly influenced by nitrogen doping. The nitrogen-doped N-3DPCN effectively captures Fe atoms, creating single-atom dispersed Fe–N$_x$ active sites, which facilitate the formation of Fe–N bonds between nitrogen and iron atoms (Figure 3h). This bonding structure is crucial for

stabilizing the dispersion of single-atom iron, preventing its aggregation into Fe$_3$N. Additionally, nitrogen atoms introduce various nitrogen functional groups within the 3D carbon network, which enhance the interfacial coupling between Fe$_3$N and N-3DPCN. This coupling effect not only increases the contact area between Fe$_3$N and N-3DPCN but also reduces the interfacial resistance, ensuring efficient electron and ion transfer. Moreover, this strong interfacial coupling preserves the structural integrity of the electrode under high current densities, preventing material aggregation or detachment during prolonged cycling. During discharge, Fe$_3$N converts into atomically dispersed iron (SAFe–N@3DPCN) (Figure 3i), which catalyzes the rapid reduction of the discharge product Na$_3$N on the electrode surface to Na$_2$N and Na, thereby extending the battery's cycle life. Therefore, future research on 3D carbon materials in alkali metal ion batteries should further explore nitrogen doping strategies to fine-tune the structural properties of 3D porous carbon materials, with the goal of enhancing their cycle stability.

Batteries & Supercaps

Review

doi.org/10.1002/batt.202400563

Chemistry
Europe

European Chemical
Societies Publishing

3.2. Alkali Metal Sulfur Batteries

Unlike alkali metal ion batteries, sulfur batteries encounter the severe issue of the polysulfide shuttle effect during charge-discharge process, resulting in rapid capacity decay and decreased efficiency. For example, in lithium-sulfur batteries, lithium polysulfides (LiPSs) can convert into poorly conductive, insoluble Li_2S and Li_2S_2, significantly increasing the battery's internal resistance and impacting its performance. 3D structures offer abundant active sites and efficient conductive pathways, which can effectively convert and immobilize LiPSs, thereby reducing their dissolution and diffusion in the electrolyte. Furthermore, these active sites can be utilized to load various catalysts for LiPSs adsorption. For this problem, researchers have introduced a 3D porous carbon structure, embedding single-atom catalysts into nitrogen-doped porous carbon to promote polysulfide conversion and mitigate the shuttle effect in sulfur batteries.[17] Additionally, phosphorus-doped 3D networks were proposed to provide adsorption sites that effectively capture polysulfides, reduce their dissolution and diffusion, and promote Li–S bond cleavage, thereby accelerating polysulfide conversion reactions.[18]

Hence, utilizing 3D porous carbon materials to load catalysts can simultaneously adsorb polysulfides, enhance conductivity, and lower reaction barriers, thus more effectively suppressing polysulfide conversion. Shi et al. reported a CoP@NPC composite material characterized by abundant foam-like pores and an interconnected network structure (Figure 4a).[19] The material exhibits a high degree of graphitization with fewer defects (Figure 4d) and a well-developed pore structure, which contributes to a larger specific surface area. Moreover, CoP nanoparticles, approximately 20 nanometers in size, are uniformly embedded within the nitrogen-phosphorus co-doped porous carbon matrix (NPC) (Figure 4b and c). These nanoparticles are anchored to the NPC surface, enhancing the material's electrocatalytic activity and leading to superior electrochemical performance. Similarly, Jia et al. reported a material with niobium single-atom catalysts (Nb-SAs) embedded in 3D ordered porous carbon nanofibers (3DOP–C), serving as a sulfur host for lithium-sulfur batteries.[20] 3D porous material offers increased surface area and pore volume to enhance sulfur loading, while its inherent conductivity helps mitigate the conductivity loss caused by Li_2S deposition. Additionally, the uniform dispersion of Nb atomic catalysts across the carbon nanofibers enhances the material's conductivity and interfacial activity, while also significantly improving its ability to adsorb and convert polysulfides. Density functional theory (DFT) calculations reveal that the adsorption energy of Li_2S_6 on Nb-SAs@3DOP–C (-1.09 eV) is significantly higher than on 3DOP–C (-0.124 eV), indicating a notable advantage of Nb-SAs@3DOP–C in chemically adsorbing polysulfides. Based on calculated Gibbs free energy, the adsorption of Nb in Nb-SAs@3DOP–C results in lower reaction free energy (Figure 4e), indicating that the deposition and decomposition of
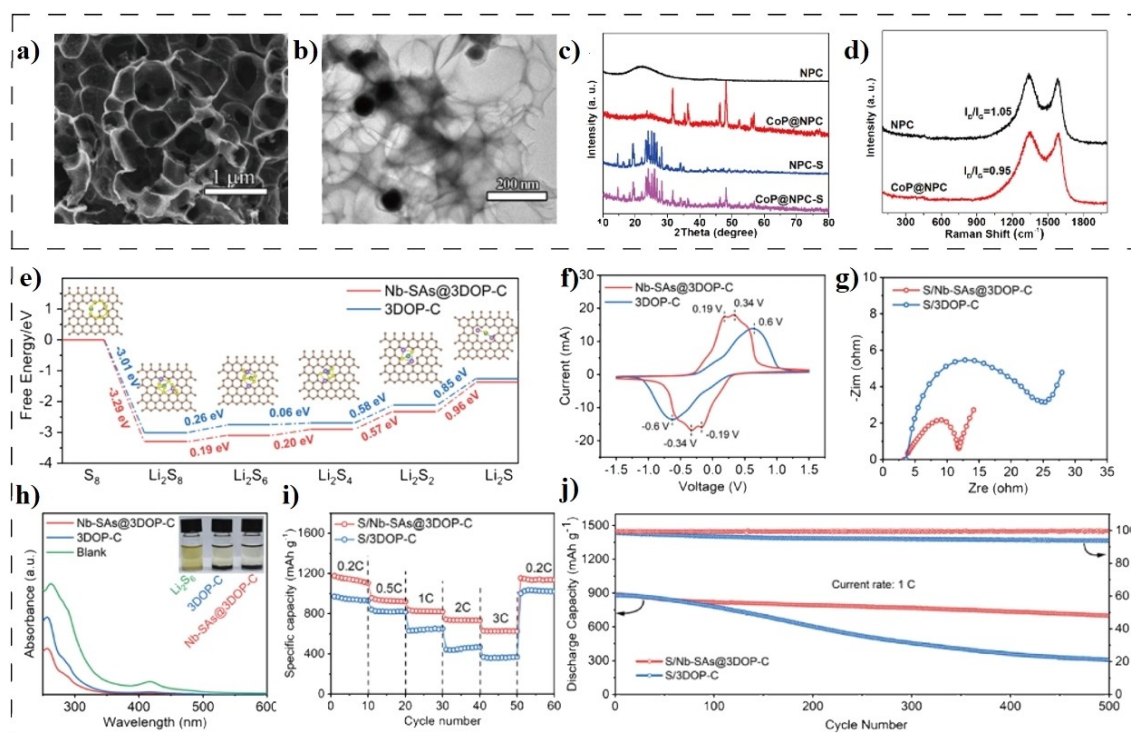

Figure 4. (a) SEM images of CoP@NPC. (b) TEM images of CoP@NPC. (c) XRD patterns of NPC, CoP@NPC, NPC–S, and CoP@NPC–S. (d) Raman shift of NPC and CoP@NPC. Reproduced with permission.[19] Copyright 2023, American Chemical Society. (e) Gibbs free energy spectra of LiPSs on Nb-SAs@3DOP–C and 3DOP–C nanofibers. (f) Cyclic voltammetry tests of Nb-SAs@3DOP–C and 3DOP–C. (g) EIS tests of S/Nb-SAs@3DOP–C and S/3DOP–C. (h) UV-vis spectra and optical observations (inset) of polysulfide solutions adsorbed by Nb-SAs@3DOP–C and 3DOP–C nanofibers. (i) Rate performance of S/Nb-SAs@3DOP–C. (j) Cycling performance and Coulombic efficiency of S/Nb-SAs@3DOP–C and S/3DOP–C electrodes. Reproduced with permission.[20] Copyright 2024, Elsevier B.V.

Batteries & Supercaps

Review
doi.org/10.1002/batt.202400563

Chemistry Europe
European Chemical
Societies Publishing

Li_2S in Nb-SAs@3DOP—C are thermodynamically more favorable, thereby accelerating the overall electrochemical conversion process. Cyclic voltammetry (CV) tests (Figure 4f) revealed that the Nb-SAs@3DOP—C electrodes exhibit sharper redox peaks and lower overpotential, indicating higher catalytic activity. Additionally, EIS tests (Figure 4g) showed lower charge transfer resistance, demonstrating its superiority in catalyzing polysulfide conversion. Furthermore, a comparison of the adsorption phenomena of Nb-SAs@3DOP—C and 3DOP—C in Li_2S_6 solution (Figure 4h) showed that Nb-SAs@3DOP—C can more effectively capture LiPSs. These findings indicate that the Nb-SAs@3DOP—C composite could play an efficient role in blocking the polysulfide shuttle effect. The electrochemical performance of this material is quite excellent, its discharge capacity at 0.2 C reached 1208.1 mAh g^{-1} (Figure 4i). Not only that, the material's long-cycle stability is quite excellent, with an average decay rate of only 0.012% per cycle after 500 cycles at 1 C (Figure 4j), which confirms its potential as a positive electrode material for high-performance lithium-sulfur batteries.

Consequently, future research on sodium-sulfur batteries should remain focused on strategies to mitigate the polysulfide shuttle effect. This can be accomplished by incorporating more effective catalysts into 3D materials, which can adsorb polysulfides and prevent their shuttling within the electrolyte.

3.3. Alkali Metal Air Batteries

Alkali metal-air batteries show significant potential for energy storage and conversion. However, their practical applications face many challenges. Chief among these is cycle stability. The direct participation of oxygen from the air in reactions leads to irreversible chemical changes in the electrode materials during charge and discharge cycles, resulting in a passivation layer on the electrode surface that degrades battery performance.[21] Additionally, the reaction products (e.g. lithium oxide, lithium peroxide) in alkali metal-air batteries tend to deposit on the electrode surface, this layer increases internal resistance and reduces both capacity and energy efficiency.[16] To tackle these challenges, 3D porous carbon materials capable of loading catalysts are essential. Researchers have developed Fe—N—C catalysts with enhanced oxygen reduction reaction (ORR) activity by inserting metal potassium into 3D porous carbon to create more defect sites and fix single iron atoms.[21] Alternatively, nitrogen-doped 3D porous carbon nanosheets have been used to create bifunctional catalysts for oxygen reduction and oxygen evolution in zinc-air batteries.[16]

If other heteroatoms that can enhance catalytic efficiency are introduced based on nitrogen doping, more efficient catalysts can be obtained. Guided by DFT calculations (Figure 5a), Wang et al. introduced a novel strategy to enhance the internal dynamics of air batteries by tuning the p-band center, resulting in the preparation of N and S co-doped porous carbon

with an ultra-thin mesh structure (Figure 5b and c).[14] The 3D porous carbon structure significantly increases the electrode's specific surface area, facilitating greater CO_2 adsorption onto the electrode surface, thus accelerating electrochemical reaction rates. Additionally, it exposes more active sites, effectively catalyzing CO_2 reduction and evolution reactions. Simultaneously, the co-doping of N and S tunes the p-band center of the 3D porous carbon to an optimal −3.85 eV (Figure 5d). This optimal p-band center balances adsorption energy, significantly reducing the formation and decomposition of Na_2CO_3, enabling faster conversion of intermediates like Na_2CO_3. Moreover, this hybridization enhances the interaction between Na_2CO_3 and the catalyst surface, stabilizing Na_2CO_3 adsorption and optimizing intermediate formation and decomposition processes. Analyzing the decomposition pathways and energy barriers of Na_2CO_3 on various doped graphenes (N—G, NS—G, S—G), NS—G exhibits the lowest energy barrier (2.41 eV), demonstrating that the synergistic effect of N and S renders NS—G the most effective catalyst for Na_2CO_3 formation and decomposition (Figure 5e). Therefore, under the combined influence of 3D porous materials and catalysts, NS-PC/CP exhibits the lowest charge voltage and the highest discharge voltage (Figure 5f), resulting in the smallest voltage difference (Figure 5g). This indicates higher reaction efficiency and minimal energy loss within the battery. Moreover, this NS-PC/CF battery demonstrates strong flexibility, with rate performance tests in both flat and bent states showing considerable stability (Figure 5h).

Although 3D porous carbon and its composites have many advantages in terms of battery electrode materials. However, many challenges remain. For example, the wide contact area between the 3D porous carbon material and the electrolyte promotes the formation of a thick solid electrolyte interface (SEI), which can cause significant irreversible capacity loss during the initial cycle. Therefore, 3D porous carbon materials still need to improve long-term cycle stability. Based on the above drawbacks, we think future studies should focus on exploring additional doping elements that can bond with nitrogen and exhibit potential catalytic activity. It will be important to investigate how different elements, in varying proportions, impact the catalytic performance of 3D porous carbon materials. Additionally, optimizing theoretical calculation techniques to accurately regulate the electronic structure and active site distribution in electrode materials will be crucial. Such advancements are expected to enhance the overall cycle stability of air batteries.

4. Application for Supercapacitors

Supercapacitors and batteries are the two most concerned electrochemical energy storage devices today.[22] Compared with batteries, supercapacitors have high power density, long cycle life, rapid charging, good discharging interval.[23] Supercapacitors are divided into electrical double-layer capacitors, pseudocapacitors, and Asymmetric supercapacitors.[24] No matter what kind of supercapacitor, it needs higher capaci-
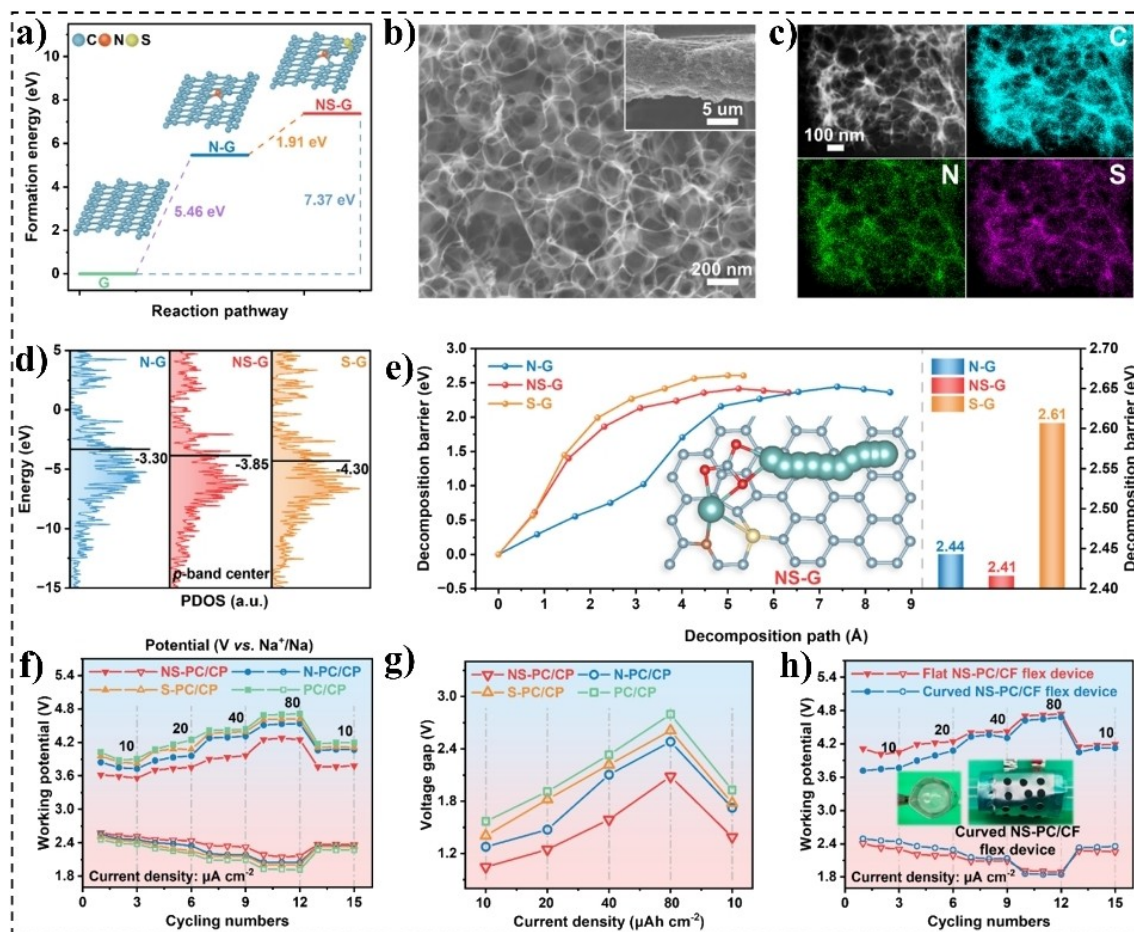
Batteries & Supercaps

Review
doi.org/10.1002/batt.202400563

Chemistry Europe
European Chemical
Societies Publishing

Figure 5. (a) The formation energies of NS—G with one-step and two-step reaction pathways. (b) The SEM image of NS-PC, (c) The EDS-mapping images showing the distribution of C, N, and S elements in NS-PC/CP. (d) The partial density of states (PDOS) for p orbitals of N–G, NS–G, and S–G. (e) The decomposition barriers of the initial Na–O bond fracture and desodiation on N–G, NS–G, and S–G. The inset in (e) shows detailed decomposition paths of Na_2CO_3 on the NS–G catalyst. (f) Discharging and charging voltages at different current densities for the four cathodes and (g) voltage gaps at different current densities of the four cathodes. (h) Discharging and charging voltages at different current densities of the NS-PC/CF flexible device under different mechanical states. The insets show digital photos of the device in a curved state. Reproduced with permission.[14] Copyright 2024, Elsevier B.V.

tance and faster charge and discharge speed to adapt to new needs. 3D porous carbon materials have high specific surface area and high conductivity. It is an ideal material for making electrode material.

4.1. Electrical Double-Layer Capacitors

Electrical double-layer capacitors (EDLCs) are designed by adsorbing ions to the electrode surface and it storing charge in an electrostatic manner.[2d] The large specific surface area of carbon materials makes it well-suited for ion adsorption.[25] However, uncontrolled pore sizes can hinder effective ion transfer. The 3D porous carbon produced via the salt-template method offers adjustable pore size and distribution, significantly enhancing the energy storage capacity of super-capacitors.

Zhu et al. employed a straightforward one-pot method, utilizing the self-assembly of various water-soluble NaX salts, which connect NaCl, Na_2CO_3 and Na_2SiO_3, as structure-

directing templates, to synthesize 3D hierarchical porous carbons (Figure 6a). The 3D carbon with tailored pore size distribution has both high specific surface area and fast ion transport. This material exhibited a high specific capacitance of $320\,F\,g^{-1}$ at $0.5\,A\,g^{-1}$ and an outstanding high rate capacitance retention of $126\,F\,g^{-1}$ at $200\,A\,g^{-1}$ (Figure 6b–d).[10] 2D carbon materials generally allow for faster ion transport compared to 3D ones. Based on this, Zhu et al. addressed the material by assembling two-dimensional carbon nanosheets with tailored pore size distribution into a 3D porous carbon structure (Figure 6e and f). This material features a large number of mesopores, facilitating efficient ion transport. Additionally, nitrogen doping was incorporated into the 3D porous carbon, enhancing capacity through additional Faradaic redox reactions, thus achieving a pseudo-capacitive effect (Figure 6g).[26] This material exhibited a specific capacitance of $225\,F\,g^{-1}$ at $1\,A\,g^{-1}$ (Figure 6h).[7b]

As research progresses, it has become clear that a single carbon nanostructure rarely meets all the requirements for high specific surface area, stable structure, high conductivity,
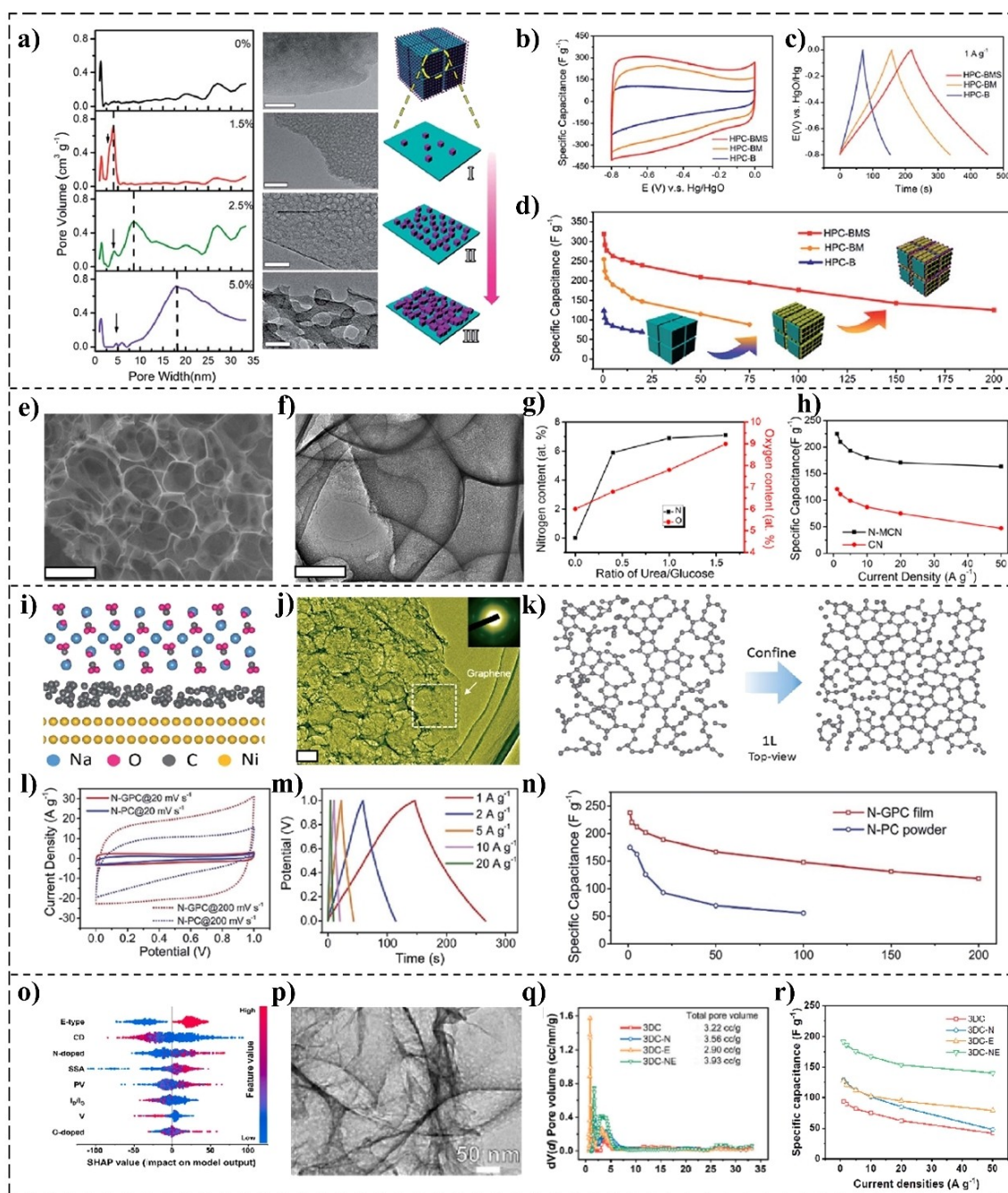
Figure 6. (a) Pore size distributions and the corresponding TEM images of hierarchical porous carbons-big and small pores (HPC-BS) based on different mass ratios of Na_2SiO_3 to NaCl from 0%, 1.5% to 2.5% and 5% (the scale bars are 50 nm) and Scheme of the morphology evolution of combination templates; Electrochemical performance of hierarchical porous carbons-big pores (HPC–B), hierarchical porous carbons-big and medium pores (HPC-BM) and hierarchical porous carbons-big, medium, and small pores (HPC-BMS) measured in a three-electrode system; (b) CV curves at a scan rate of 5 mV s^{-1}; (c) Charge–discharge profiles at the current density of 1 A g^{-1}; (d) Specific capacitances at different current densities. Reproduced with permission.[10] Copyright 2015, The Royal Society of Chemistry. (e) The SEM images of N-doped carbon ultrathin nanosheets with closely packed mesopores (N-MCN); (f) The TEM images of N-MCN; (g) The relation among N-doping and O-doping levels with the ratio of urea and glucose; (h) Specific capacitance of N-MCN and carbon nanosheets (CN) at various current densities. Reproduced with permission.[7b] Copyright 2016, American Chemical Society. (i) The model of heterogeneous space-confined effect; (j) TEM image of graphene-reinforced N-doping porous carbon network (N–GPC) film; (k) The top-view of one carbon atom layer with/without confined effect; (l) CV curves of N–GPC and N-doping porous carbon network (N–PC) at 20 and 200 mV s^{-1}; (m) GCD profiles of N–GPC at various current densities; (n) specific capacitance of N–GPC and N–PC powder at various current densities. Reproduced with permission.[13] Copyright 2017, The Royal Society of Chemistry. (o) Shapley Additive Explanations (SHAP) analysis honeycomb diagram for each feature; (p) Morphology characterization: SEM image of 3D network carbon material with KOH etching and N-doping (3DC-NE); (q) Pore size distribution of 3D network carbon material (3DC) samples; (r) Specific capacitances of samples at various current densities according to the GCD test. Reproduced with permission.[27] Copyright 2022, Elsevier B.V.

and fast ion conduction. For instance, graphene, a typical 2D structure, offers excellent electron conductivity and mechan-ical properties but is prone to agglomeration. On the other hand, 3D carbon networks provide efficient mass transport

Batteries & Supercaps

Review

doi.org/10.1002/batt.202400563

Chemistry Europe

European Chemical
Societies Publishing

but can be susceptible to structural collapse.[13] Carbon hybrids, which combine two or more carbon allotropes, exhibit enhanced electrical and mechanical properties at the nanoscale compared to simple mixtures. Zhu et al. constructed a composite structure by integrating two-dimensional graphene with 3D porous carbon (Figure 6i and j). The 2D carbon material, formed under confined conditions, developed a more regular structure (Figure 6k), improving the material's electrical conductivity and mechanical stability. She also doped the carbon material with nitrogen, which further increased the specific capacitance of the supercapacitor. It exhibited a specific capacitance of 238 F g^{-1} at 1 A g^{-1} (Figure 6l–n).[13] As a new carbon material, biomass-derived porous carbon has high specific surface area, abundant pores, nitrogen, phosphorus and other elements. Moreover, it has wide sources and low cost, and is suitable for preparing supercapacitor electrode materials. Zhang et al. utilized biomass sources to prepare 3D porous carbon, which exhibited a specific capacitance of 103 F g^{-1} at 0.1 A g^{-1}.[28]

Traditional materials design methods often rely on empirical knowledge. However, machine learning can significantly enhance material design by analyzing large datasets to identify key factors influencing supercapacitor performance. Wang et al. used machine learning to determine that nitrogen content and specific surface area have the most significant impact on the specific capacitance of supercapacitors (Figure 6o). Based on this insight, they designed a 3D porous carbon material with high specific surface area and elevated nitrogen content (Figures 6p and q), resulting in a specific capacitance of 191.2 F g^{-1} at 1 A g^{-1} (Figure 6r).[27] Tailoring pore size distribution is crucial for optimizing 3D porous carbon materials for supercapacitors.[10] Enhancing these materials by incorporating nitrogen or combining them with two-dimensional materials can significantly improve their energy storage performance. In recent years, machine learning has provided a more scientific approach to designing 3D porous carbon, allowing for more targeted and efficient preparation processes.

4.2. Pseudocapacitors

Pseudocapacitors are used to store energy electrochemically via rapid surface-controlled redox reactions, which is different from electrical double-layer capacitors.[29] Pseudocapacitor materials are faced with problems such as easy agglomeration and poor electrical conductivity. 3D porous carbon, with its excellent electrical conductivity and well-structured pores, offers an ideal solution for loading pseudocapacitive materials. Therefore, it is feasible to create 3D porous carbon composite pseudocapacitive materials for use as pseudocapacitor electrodes.

VS$_2$, for example, has a high theoretical specific capacity, making it a promising candidate for pseudocapacitor electrodes. However, issues such as severe aggregation, structural damage, reduced capacity, poor cycling stability, and limited rate capability hinder its practical application.[30] To address

these challenges, Feng et al. developed 3D porous carbon composite VS$_2$ materials using a combination of freeze-drying and annealing with NaCl salt-templates (Figure 7a). The incorporation of 3D porous carbon helps to mitigate the agglomeration and aging of VS$_2$, reduces volume expansion during reactions, and enhances the capacitance contribution of VS$_2$ (Figure 7b and c).[30] Co-based zeolitic imidazolate framework (ZIF-67) is another pseudocapacitive material, but its low conductivity and poor ion transport capacity limit its practical application. To overcome these challenges, Deng et al. combined ZIF-67 with 3D porous carbon to create enhanced electrode materials (Figure 7d and e). The 3D porous carbon serves as nucleation sites for ZIF-67, establishes conductive networks, and restricts the growth of ZIF-67 crystals (Figure 7f). This integration addresses the issues of poor conductivity and slow ion transport in ZIF-67, resulting in a specific capacitance of 119 F g^{-1} at 0.5 A g^{-1} (Figure 7g–i).[31] In summary, the stabilization of pseudocapacitive material structures within 3D porous carbon provides an effective conductive network and serves as an excellent carrier for improving performance.

5. Conclusion and Outlooks

3D porous carbon has been widely used in various electrochemical energy storage devices because of its high specific surface area, good electrical conductivity and abundant pore structure. This review summarizes the preparation of 3D porous carbon by salt template method and its application in energy storage devices such as alkali metal-ion batteries, alkali metal-sulfur batteries, alkali metal-air batteries and supercapacitors. Recent advances in this field are also discussed, with emphasis on the relationship between pore structure and electrochemical properties of porous carbon.

The review delved into the self-assembly methods used for synthesizing porous carbon precursors through the salt-template method, such as low-temperature freeze-drying, room-temperature anti-solvent techniques, and high-temperature spray drying. These methods allow for flexible control over the structure, pore size, and morphology of 3D porous carbon and its composites by selecting appropriate parameters, including the type and size of the template. To address the issue of powdered carbon material aggregation, which impedes ion transport within electrodes, researchers have developed self-standing electrodes through hot pressing or by combining the carbon with metal or alternative material substrates. This design approach enables 3D porous carbon materials to exhibit remarkable electrochemical properties across a range of energy storage devices, offering promising prospects for future applications.

However, despite the excellent electrochemical properties of 3D porous carbon and its composites, several challenges remain in practical applications (Figure 8). Firstly, the removal of the salt template after carbonization still requires the use of corrosive liquids, such as strong acids and bases. The disposal of these liquids poses environmental risks and
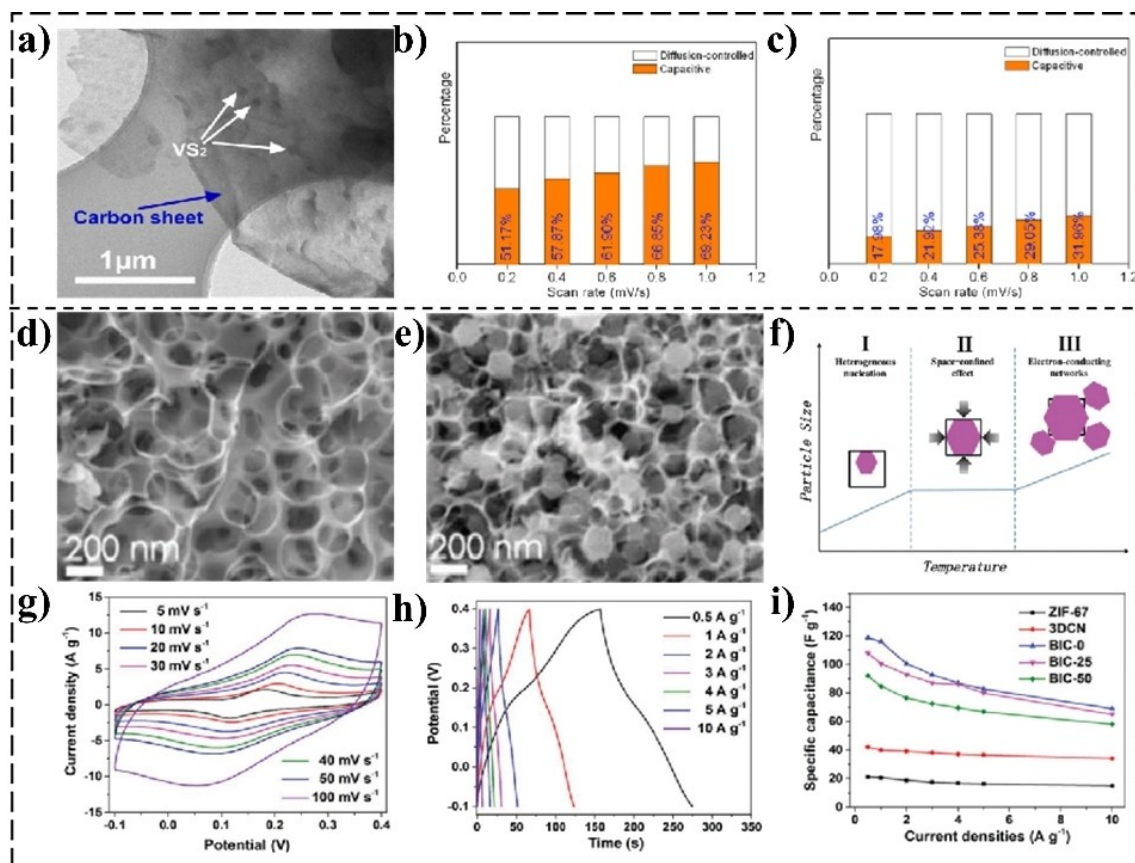
Figure 7. (a) TEM image of VS_2-carbon composite (VS_2-NC); (b) bare VS_2 and (c) VS_2-NC. Reproduced with permission.[30] Copyright 2022, Elsevier Ltd and Techna Group S.r.l. (d) SEM images of 3D carbon network (3DCN) and (e) ball-in-cage nanostructure (BIC-0); (f) Three functions of 3DCN in the fabrication of BIC; (g) CV plots of the BIC-0 electrode at different scan rates from 5 mV s^{-1} to 100 mV s^{-1}; (h) GCD curves of BIC-0 at different current densities; (i) Specific capacitances of 3DCN, ZIF-67 and ball-in-cage nanostructure which reaction temperatures was 0 °C, 25 °C and 50 °C (BIC-0/25/50) electrodes calculated from GCD curves. Reproduced with permission.[31] Copyright 2017, The Royal Society of Chemistry.
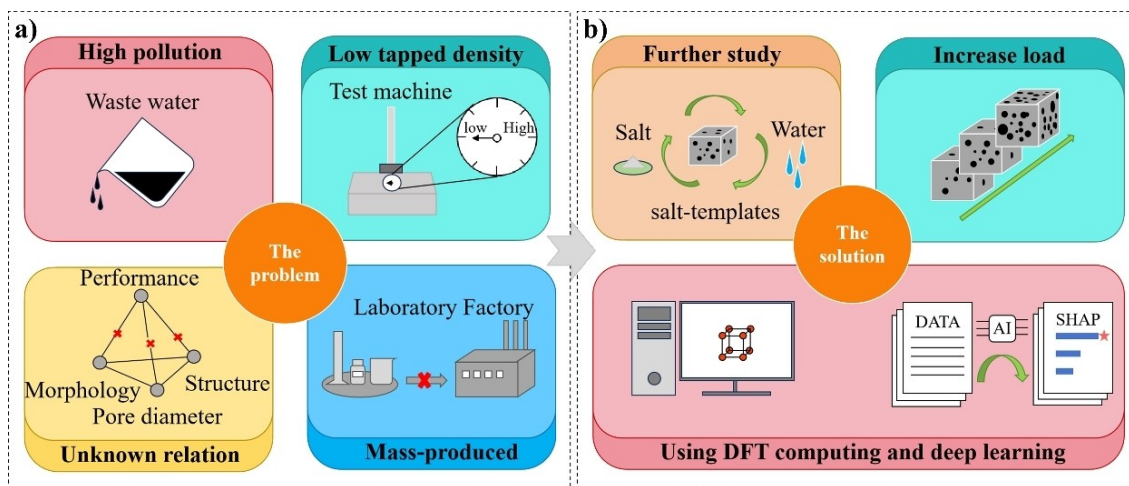

Figure 8. (a) The problems in the design and (b) possible solutions and future directions of 3D porous carbon materials.

increases production costs. Secondly, while the porous structure enhances ion diffusion dynamics and exposes more active sites, it also reduces the vibrational density, which negatively impacts the energy and power density of batteries. Thirdly, the complex interrelationships between a material's intrinsic properties—such as structure, pore size, morphology, and electrochemical performance—are not yet fully understood, hindering the development of reliable design guidelines. Lastly, the preparation of 3D porous carbon remains limited to laboratory-scale production, and

scaling up for industrial applications presents an unresolved challenge. Addressing these challenges is crucial for advancing the practical application of 3D porous carbon in energy storage technologies.

Despite the challenges associated with 3D porous carbon, there are significant opportunities for advancement. First, the environmental impact of template removal must be addressed. Developing a green, pollution-free salt-template preparation method is essential to mitigate this issue. Second, to address the low energy density of batteries, it is crucial to increase the mass loading of active material while maintaining rapid ion migration and abundant active sites. This requires the exploration of innovative and effective design strategies. Third, the intricate relationship between structure, pore size, morphology, and the electrochemical properties of 3D porous carbon materials remains poorly understood. This presents challenges in the discovery of new materials, structures, and methods. However, theoretical computation and machine learning have begun to make progress in understanding electrode material design and reaction mechanisms.[32] Leveraging these tools to guide the design of 3D porous carbon may yield unexpected benefits. We believe that with continued research and development, the application of salt templates in the preparation of 3D porous carbon will evolve, unlocking greater potential to meet the demands of a wider range of energy storage applications.

Acknowledgements

Conflict of Interests

The authors declare that they have no known competing financial interests or personal relationships that could have appeared to influence the work reported in this paper.

Data Availability Statement

The data that support the findings of this study are available from the corresponding author upon reasonable request.

[1] a) X. Dou, I. Hasa, D. Saurel, C. Vaalma, L. Wu, D. Buchholz, D. Bresser, S. Komaba, S. Passerini, *Mater. Today* **2019**, *23*, 87; b) C. Jiang, B. Chen, M. Xu, J. Jiang, *Energy Storage Mater.* **2024**, *70*, 103518; c) M. Huang, M. Wang, L. Yang, Z. Wang, H. Yu, K. Chen, F. Han, L. Chen, C. Xu, L. Wang, P. Shao, X. Luo, *Nano Micro Lett.* **2024**, *16*, 207; d) P. Zhang, W. Zhang, Z. Wang, X. Wang, Q. Ren, S. Zhang, Y. Wang, L. He, P. Liu, Q. Zhang, Z. Shi, *eScience* **2023**, *3*, 100184; e) B. Chen, D. Wang, B. Zhang, X. Zhong, Y. Liu, J. Sheng, Q. Zhang, X. Zou, G. Zhou, H. Cheng, *ACS Nano* **2021**, *15*, 9841; f) B. Chen, D. Chao, E. Liu, M. Jaroniec, N. Zhao, S. Qiao, *Energy Environ. Sci.* **2020**, *13*, 1096; g) B. Chen, T. Wang, S. Zhao, J. Tan, N. Zhao, S. P. Jiang, Q. Zhang, G. Zhou, H. M. Cheng, *Adv. Mater.* **2021**, *33*, 2007090; h) T. Ji, X. Liu, T. Zhang, Y. Shi, D. Sheng, H. Yin, Z. X. Shen, D. Chao, *Adv. Energy Mater.* **2024**, 14, 2401908; i) W. Z. Huang, P. Xu, X. Y. Huang, C. Z. Zhao, X. Bie, H. Zhang, A. Chen, E. Kuzmina, E. Karaseva, V. Kolosnitsyn, X. Zhai, T. Jiang, L. Z. Fan, D. Wang, Q. Zhang, *MetalMat* **2023**, *1*, e6; j) Q. Wang, W. Zhou, Y. Zhang, H. Jin, X. Li, T. Zhang, B. Wang, R. Zhao, J. Zhang, W. Li, Y. Qiao, C. Jia, D. Zhao, D. Chao, *Natl. Sci. Rev.* **2024**, 11, nwae230.

[2] a) Z. Liu, J. Ma, M. Hong, R. Sun, *ACS Catal.* **2023**, *13*, 2106; b) J. Liu, X. Li, B. Jin, H. Tang, L. Ma, R. Zhang, J. Ran, H. Zhang, *Chem. Eng. J.* **2022**, *441*, 136052; c) Q. Wu, B. Chen, H. Xie, X. Bai, M. Liang, Z. Wu, X. Jin, C. He, N. Zhao, *Chem. Eng. J.* **2022**, *430*, 132906; d) X. Deng, J. Li, L. Ma, J. Sha, N. Zhao, *Mater. Chem. Front.* **2019**, *3*, 2221; e) N. Wei, L. Yu, Z. Sun, Y. Song, M. Wang, Z. Tian, Y. Xia, J. Cai, Y. Li, L. Zhao, Q. Li, M. H. Rümmeli, J. Sun, Z. Liu, *ACS Nano* **2019**, *13*, 7517; f) C. Chen, C. Lee, Y. Tang, *Nano Micro Lett.* **2023**, *15*, 121; g) H. Xie, B. Chen, C. Liu, G. Wu, S. Sui, E. Liu, G. Zhou, C. He, W. Hu, N. Zhao, *Energy Storage Mater.* **2023**, *60*, 102830; h) Y. Chen, C. Lu, *Carbon Neutralization* **2023**, *2*, 585

[3] a) X. Zhang, N. Zhao, C. He, *Prog. Mater. Sci.* **2020**, *113*, 100672; b) B. Chen, S. Sui, F. He, C. He, H. Cheng, S. Qiao, W. Hu, N. Zhao, *Chem. Soc. Rev.* **2023**, *52*, 7802.

[4] a) M. Liang, L. Ma, B. Chen, E. Liu, C. Shi, C. He, N. Zhao, *Energy Storage Mater.* **2022**, *47*, 591; b) Q. Zhai, H. Huang, T. Lawson, Z. Xia, P. Giusto, M. Antonietti, M. Jaroniec, M. Chhowalla, J. B. Baek, Y. Liu, S. Qiao, L. Dai, *Adv. Mater.* **2024**, *36*, 2405664.

[5] a) S. Zhu, N. Zhao, J. Li, X. Deng, J. Sha, C. He, *Nano Today* **2019**, *29*, 100796; b) S. Sui, H. Xie, B. Chen, T. Wang, Z. Qi, J. Wang, J. Sha, E. Liu, S. Zhu, K. Lei, S. Zheng, G. Zhou, C. He, W. Hu, F. He, N. Zhao, *Angew. Chem. Int. Ed.* **2024**, *63*, e202411255.

[6] a) B. Chen, D. Wu, T. Wang, F. Yuan, D. Jia, *Chem. Eng. J.* **2023**, *462*, 142163; b) Y.-S. Liu, C. Ma, K.-X. Wang, J. Chen, *New Carbon Mater.* **2023**, *38*, 1; c) J. Li, H. Yu, Y. Lv, Z. Cai, Y. Shen, L. Ruhlmann, L. Gan, M. Liu, *Nanotechnology* **2024**, *35*, 152001; d) Y. Qin, S. Jha, C. Hu, Z. Song, L. Miao, Y. Chen, P. Liu, Y. Lv, L. Gan, M. Liu, *J. Colloid Interface Sci.* **2024**, *675*, 1091–1099; e) D. Zhang, L. Miao, Z. Song, X. Zheng, Y. Lv, L. Gan, M. Liu, *Energy & Fuels* **2024**, *38*, 12510.

[7] a) Y. Shu, X. Duan, Q. Niu, R. Xie, P. Zhang, Y. Pan, Z. Ma, *Chem. Eng. J.* **2021**, *426*, 131757; b) S. Zhu, J. Li, L. Ma, L. Guo, Q. Li, C. He, E. Liu, F. He, C. Shi, N. Zhao, *ACS Appl. Mater. Interfaces* **2016**, *8*, 11720; c) M. Liang, H. Xie, E. Liu, C. Shi, C. He, N. Zhao, *Carbon* **2022**, *196*, 795; d) B. Chen, J. Ding, X. Bai, H. Zhang, M. Liang, S. Zhu, C. Shi, L. Ma, E. Liu, N. Zhao, F. He, W. Zhou, C. He, *Adv. Funct. Mater.* **2021**, *32*,2109899.

[8] a) B. Chen, H. Li, H. Liu, X. Wang, F. Xie, Y. Deng, W. Hu, K. Davey, N. Zhao, S. Z. Qiao, *Adv. Energy Mater.* **2019**, *9*, 1901146; b) B. Chen, H. Lu, J. Zhou, C. Ye, C. Shi, N. Zhao, S. Z. Qiao, *Adv. Energy Mater.* **2018**, *8*, 1702909; c) B. Chen, Y. Meng, F. Xie, F. He, C. He, K. Davey, N. Zhao, S. Z. Qiao, *Adv. Mater.* **2018**, *30*, 1804116; d) B. Chen, X. Zhong, G. Zhou, N. Zhao, H. M. Cheng, *Adv. Mater.* **2021**, *34*, 2105812.

[9] B. Chen, Z. Qi, B. Chen, X. Liu, H. Li, X. Han, G. Zhou, W. Hu, N. Zhao, C. He, *Angew. Chem. Int. Ed.* **2023**, *63*, e202316116.

[10] S. Zhu, J. Li, C. He, N. Zhao, E. Liu, C. Shi, M. Zhang, *J. Mater. Chem. A* **2015**, *3*, 22266.

[11] J. Qin, H. M. Kheimeh Sari, C. He, X. Li, *J. Mater. Chem. A* **2019**, *7*, 3673.

[12] a) M. Liang, H. Zhang, B. Chen, X. Meng, J. Zhou, L. Ma, F. He, W. Hu, C. He, N. Zhao, *Adv. Mater.* **2023**, *35*, 2307209; b) C. Liu, H. Xie, S. Sui, B. Chen, L. Ma, E. Liu, N. Zhao, *Mater. Today Energy* **2022**, *26*, 100993.

[13] S. Zhu, K. Xu, S. Sui, J. Li, L. Ma, C. He, E. Liu, F. He, C. Shi, L. Miao, J. Jiang, N. Zhao, *J. Mater. Chem. A* **2017**, *5*, 19175.

[14] Y. Wang, Y. Cheng, B. Chen, J. Zhou, H. Xie, Y. Fan, J. Sha, E. Liu, F. He, C. He, W. Hu, N. Zhao, *Energy Storage Mater.* **2024**, *71*, 103655.

[15] M. Liang, H. Xie, B. Chen, H. Qin, H. Zhang, J. Wang, J. Sha, L. Ma, E. Liu, J. Kang, C. Shi, F. He, X. Han, W. Hu, N. Zhao, C. He, *Angew. Chem. Int. Ed.* **2024**, *63*, e202401238.

[16] M. Ding, X. Hui, L. Yin, *Electrochim. Acta* **2023**, *468*, 142891.

Batteries & Supercaps

Review
doi.org/10.1002/batt.202400563

Chemistry Europe
European Chemical
Societies Publishing

[17] a) S. Ju, C. Yuan, J. Zheng, L. Yao, T. Zhang, G. Xia, X. Yu, *Energy Storage Mater.* **2022**, *52*, 524; b) Y. Su, X.-Y. Liu, R. Zhang, S. Zhang, J. Wang, Y.-D. Qian, Z.-C. Jian, Y.-F. Zhu, J.-F. Mao, S. Xu, S. Dou, Y. Xiao, *Energy Storage Mater.* **2024**, *71*, 103638.

[18] F. Liu, N. Wang, C. Shi, J. Sha, L. Ma, E. Liu, N. Zhao, *Chem. Eng. J.* **2022**, *431*, 133923.

[19] Z. Shi, J. Xu, Y. Wang, Y. Pang, W. Zhao, H. Yue, Z. Yang, S.-T. Yang, Y. Yin, *ACS Sustainable Chem. Eng.* **2023**, *11*, 16267.

[20] S. Jia, S. Zhao, Z. Xu, C. Ma, T. Yang, L. Pan, J. Liu, Y. Wang, T. Zhang, X. Sun, N. Liu, Y. Zhang, Z. Chen, *Appl. Catal. B: Environ. Energy* **2024**, *351*, 124012.

[21] a) M. Arif Khan, C. Sun, J. Cai, D. Ye, K. Zhao, G. Zhang, S. Shi, L. Ali Shah, J. Fang, C. Yang, H. Zhao, S. Mu, J. Zhang, *ChemElectroChem* **2021**, *8*, 1298; b) X. Ye, W. Liu, Y. Lu, X. Zheng, Y. Bi, M. Zheng, L. Han, B. Liu, Y. Ning, S. H. M. Jafri, X. Zhao, S. He, S. Zhang, H. Li, *J. Mater. Chem. A* **2024**, *12*, 10713.

[22] a) Z. Li, D. Guo, Y. Liu, H. Wang, L. Wang, *Chem. Eng. J.* **2020**, *397*, 125418; b) Y. Liu, S. Hu, T. Hu, J. Zhang, M. Wang, M. Zhou, Z. Hou, B. He, Y. Zhang, *J. Mater. Sci.* **2024**, *59*, 15315.

[23] a) P. S. Y. GoGotSi, *Nat. Mater.* **2008**, *7*, 845.

[24] A. Muzaffar, M. B. Ahamed, K. Deshmukh, J. Thirumalai, *Renew. Sustainable Energy Rev.* **2019**, *101*, 123.

[25] G. J. Tae, Y. Kim, S. Yoo, K. S. Suh, R. S. Ruoff, *ACS Nano* **2013**, *7*, 6899.

[26] Z. Zhu, Y. Men, W. Zhang, W. Yang, F. Wang, Y. Zhang, Y. Zhang, X. Zeng, J. Xiao, C. Tang, X. Li, Y. Zhang, *eScience* **2024**, *4*, 100249.

[27] Y. Wang, J. Sha, S. Zhu, L. Ma, C. He, C. Zhong, W. Hu, N. Zhao, *J. Power Sources* **2023**, *556*, 232522.

[28] Y. Zhang, Y. Cai, T. Li, M. Wang, X. Chen, Y. Xu, *J. Mater. Sci.: Mater. Electron.* **2024**, *35*, 116.

[29] P. Bhojane, *J. Energy Storage* **2022**, *45*, 103654.

[30] S. Feng, J. Chen, L. Ma, J. Wu, J. Lin, L. Liao, X. Lu, X. Yan, S. Zeng, Y. Xi, *Ceram. Int.* **2022**, *48*, 20020.

[31] X. Deng, S. Zhu, J. Li, L. Ma, F. He, E. Liu, C. He, C. Shi, Q. Li, N. Zhao, *Nanoscale* **2017**, *9*, 6478.

[32] S. Zhu, K. Jiang, B. Chen, S. Zheng, *J. Mater. Chem. A* **2023**, *11*, 3849.